SOILS AND FOUNDATIONS Vol. 24, No. 2, 82-94, June 1984
Japanese Society of Soil Mechanics and Foundation Engineering

# A NEW MECHANICAL QUANTITY FOR SOILS AND ITS APPLICATION TO ELASTOPLASTIC CONSTITUTIVE MODELS

TERUO NAKAI* and YASUJI MIHARA**

## ABSTRACT

This paper presents a method to extend an elastoplastic constitutive model valid only in the triaxial compression condition to one applicable in general stress conditions. A stress-strain model in three-dimensional stresses was developed on the basis of the extended concept of the "Spatial Mobilized Plane" (briefly SMP*). From reconsideration of the concept of theSMP*, a mechanical quantity to describe uniquely the behavior of soils in three-dimensional stresses is obtained. This mechanical quantity $t_{ij}$ is a symmetrical tensor whose each principal value is the product of the corresponding principal stress and the corresponding direction cosine of the SMP. The mechanical quantity is then applied to the Cam-clay model as an example. It is checked by various data of drained and undrained shear tests on normally consolidated clay that the $t_{ij}$ Cam-clay model proposed here describes uniquely the behavior of soils not only under the triaxial compression condition but also under the triaxial extension and three different principal stress conditions. Although only the application of $t_{ij}$ to the Cam-clay model is shown in this paper, $t_{ij}$ is easily applicable to any other elastoplastic constitutive models for soils.

**Key words**: clay, constitutive equation of soil, dilatancy, laboratory test, shear strength, strain, stress, stress path, stress-strain curve (**IGC** : D 6)

## INTRODUCTION

Many constitutive models for soils have been proposed on the basis of the elastoplastic theories since Roscoe and his colleagues developed the original Cam-clay model (Roscoe et al., 1963; Schofield and Wroth, 1968). Most of them, however, were not generally applicable in the stress conditions except for the triaxial compression condition, because these were obtained on the basis of the elastoplastic theories of the Mises type and the validity of them was checked only by the tests under triaxial compression conditions. Since then, the models developed for triaxial compression

* Assistant Professor, Department of Civil Engineering, Nagoya Institute of Technology, Gokiso-cho, Showa-ku, Nagoya.
** Engineer, Civil Engineering Division Technology Department, Shimizu Construction Co., Ltd., 3-13, Mita, Minato-ku, Tokyo (formerly Graduate Student at Nagoya Institute of Technology).
Manuscript was received for review on September 8, 1983.
Written discussions on this paper should be submitted before January 1, 1985, to the Japanese Society of Soil Mechanics and Foundation Engineering, Sugayama Bldg. 4F, Kanda Awaji-cho 2-23, Chiyoda-ku, Tokyo 101, Japan. Upon request the closing date may be extended one month.

conditions have often been extended to those for triaxial extension conditions and/or three different principal stress conditions by modifying the soil parameters so as to satisfy Mohr-Coulomb's criterion of rupture (e. g., Roscoe and Burland, 1968), but these attempts do not seem essential.

The "Spatial Mobilized Plane (SMP)" was proposed as a plane where soil particles were considered to be most mobilized on the average in three-dimensional space, and the behavior of granular materials such as soils was analyzed after the usefulness of this plane was noticed (Matsuoka and Nakai, 1974, 1977). Furthermore, by introducing new amounts of strain increments based on the SMP, the concept of the SMP was extented in order to describe the shear behavior of soils in three-dimensional stresses more precisely (Nakai and Matsuoka, 1980, 1983 a). Then a constitutive equation for soils describing the stress-strain behavior under various stress paths in three-dimensional stresses was developed on the basis of the extended concept of the SMP and was applied to finite element analyses of soil foundations (Nakai, 1981; Nakai and Matsuoka, 1983 b). In the present paper, by generalizing the above extented concept of the SMP, a new mechanical quantity $t_{ij}$ is presented that can change any constitutive model formulated in the triaxial compression condition into one valid in general stress conditions. As an example, the proposed mechanical quantity is applied to the Cam-clay model which is one of the simplest elastoplastic constitutive equations, and the validity of the proposed model is confirmed by experimental results on a normally consolidated clay.

## DEFINITION OF THE MECHANICAL QUANTITY $t_{ij}$

A stress-strain equation under shear based on the extended concept of "Spatial Mobilized Plane (SMP)" (named SMP*) was proposed by Nakai and Matsuoka (1980, 1983 a). This equation was derived from the condition

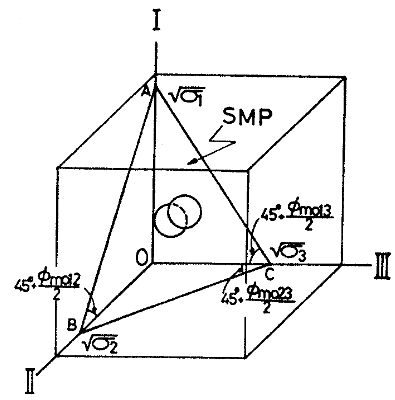


**Fig. 1. A soil element and the Spatial Mobilized Plane (ABC) in the three-dimensional space**

that there exist unique relations between the shear-normal stress ratio on the SMP ($\tau_{SMP}/\sigma_{SMP}$) and the amounts of strain increments based on the SMP ($d\varepsilon_{SMP}^*$ and $d\gamma_{SMP}^*$) under the three-dimensional stress condition. The "Spatial Mobilized Plane (SMP)" is the plane ABC in Fig. 1, where I, II and III axes represent the directions to which three principal stresses $\sigma_1$, $\sigma_2$ and $\sigma_3$ are applied, respectively. Since the values at the points where the SMP intersects these three axes are proportional to the roots of the respective principal stresses, the direction cosines ($a_1$, $a_2$ and $a_3$) of the normal to the SMP are expressed as follows (Matsuoka and Nakai, 1974);

$$a_i=\sqrt{\frac{J_3}{\sigma_i J_2}} \quad (i=1,2,3) \qquad (1)$$

Here $J_1$, $J_2$ and $J_3$ are the first, second and third effective stress invariants and expressed by the following equations using the three principal stresses.

$$\left.\begin{aligned} J_1&=\sigma_1+\sigma_2+\sigma_3\\ J_2&=\sigma_1\sigma_2+\sigma_2\sigma_3+\sigma_3\sigma_1\\ J_3&=\sigma_1\sigma_2\sigma_3\end{aligned}\right\} \qquad (2)$$

The normal and shear stresses on the SMP ($\sigma_{SMP}$ and $\tau_{SMP}$) are defined as follows.

$$\sigma_{SMP}=\sigma_1 a_1^2+\sigma_2 a_2^2+\sigma_3 a_3^2 \qquad (3)$$

$$\tau_{SMP}=\sqrt{(\sigma_1-\sigma_2)^2 a_1^2 a_2^2+(\sigma_2-\sigma_3)^2 a_2^2 a_3^2+(\sigma_3-\sigma_1)^2 a_3^2 a_1^2} \qquad (4)$$

On the other hand, the amounts of strain increments based on the SMP ($d\varepsilon_{SMP}^*$ and

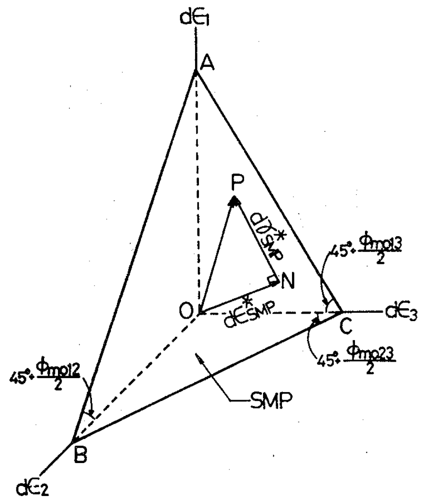


**Fig. 2. Amounts of strain increments ($d\varepsilon_{SMP}$* and $d\gamma_{SMP}$*) in the principal strain increment space**

$d\gamma_{SMP}$*) are, as shown in Fig. 2, the normal component $\overrightarrow{ON}$ and parallel component $\overrightarrow{NP}$ of the principal strain increment $\overrightarrow{OP} \equiv \overrightarrow{d\varepsilon_i} = (d\varepsilon_1, d\varepsilon_2, d\varepsilon_3)$ to the SMP (Nakai and Matsuoka, 1980, 1983 a)

$$d\varepsilon_{SMP}^* = d\varepsilon_1 a_1 + d\varepsilon_2 a_2 + d\varepsilon_3 a_3 \qquad (5)$$

$$d\gamma_{SMP}^* = \sqrt{(d\varepsilon_1 a_2 - d\varepsilon_2 a_1)^2 + (d\varepsilon_2 a_3 - d\varepsilon_3 a_2)^2 + (d\varepsilon_3 a_1 - d\varepsilon_1 a_3)^2} \qquad (6)$$

Thus, the concept of the SMP* is interpreted as the theory in which unique relations hold between the stress parameters given by Eqs. (3) and (4) and the strain increment parameters given by Eqs. (5) and (6).

In the present study, reconsidering of the concept of SMP* mentioned above, we will introduce new quantities expressed by the following equation.

$$t_i = \sigma_i \cdot a_i \quad (i = 1, 2, 3) \qquad (7)$$

If Eqs. (3) and (4) are rewritten by the use of quantities $t_i (i = 1, 2, 3)$, the normal and shear stresses ($\sigma_{SMP}$ and $\tau_{SMP}$) are represented by the following equations in the forms of the transformation of the quantities, in the same manner as ($d\varepsilon_{SMP}$* and $d\gamma_{SMP}$*) in Eqs. (5) and (6)

$$\sigma_{SMP} = t_1 a_1 + t_2 a_2 + t_3 a_3 \equiv t_N \qquad (8)$$

$$\tau_{SMP} = \sqrt{(t_1 a_2 - t_2 a_1)^2 + (t_2 a_3 - t_3 a_2)^2 + (t_3 a_1 - t_1 a_3)^2} \equiv t_S \qquad (9)$$

Therefore, the extended concept of the Spatial Mobilized Plane (SMP*) implies that there are unique relations between the normal and parallel components of $\overrightarrow{t_i} = (t_1, t_2, t_3)$ to the SMP and those of $\overrightarrow{d\varepsilon_i} = (d\varepsilon_1, d\varepsilon_2, d\varepsilon_3)$. Extending this interpretaion, if we introduce a tensor $t_{ij}$ whose principal values are $t_1$, $t_2$ and $t_3$ instead of the stress tensor $\sigma_{ij}$, it might be possible to describe uniquely the behavior of granular materials such as soils in three-dimensional stresses. Here, the principal axes of $t_{ij}$ are assumed to coincide with those of the stress.

Since the proposed mechanical quantity $t_{ij}$ is a symmetrical tensor whose principal values are $t_1$, $t_2$ and $t_3$ in Eq. (7), $t_{ij}$ can also be expressed as

$$t_{ij} = a_{ik} \cdot \sigma_{kj} \qquad (10)$$

where $\sigma_{kj}$ is the stress tensor and $a_{ik}$ is the tensor the principal values of which are given by the direction cosines ($a_1$, $a_2$ and $a_3$) of the SMP in Eq. (1). On the other hand, Satake (1982) proposed the following "second stress tensor" $\overset{*}{\sigma}_{ij}$ so as to describe the behavior of granular materials.

$$\overset{*}{\sigma}_{ij} = \frac{1}{3} \varphi_{ik}^{-1} \cdot \sigma_{kj} \qquad (11)$$

Here $\varphi_{ik}$ denotes what he called the fabric tensor of granular materials and is characterized by the frequency distribution of the interparticle contact angles originated in microscopic studies (Oda, 1972; Matsuoka, 1974). This was discussed in reference to the fabric change due to a change in stresses, so-called induced anisotropy. If we now assume that $\varphi_{ij}$ coincides with $a_{ij}^{-1}$, it is obvious from Eqs. (10) and (11) that $t_{ij}$ corresponds to $\overset{*}{\sigma}_{ij}$. In this case, it is seen from Eq. (1) that there are the following relation between the principal values of $\varphi_{ij}$ and the principal stresses,

$$\varphi_1 : \varphi_2 : \varphi_3 = \sqrt{\sigma_1} : \sqrt{\sigma_2} : \sqrt{\sigma_3} \qquad (12)$$

Eq. (12) shows that the present idea is qualitatively compatible with the experimental observation by Oda (1972) that the normals to the interparticle contacts gradually concentrate on the average in the direction of the major principal stress along with the increase in stress ratio. From the above discussion, the tensor $t_{ij}$ is considered to be a mechanical quantity reflecting the induced anisotropy of such granular materials as soils.

## APPLICATION OF $t_{ij}$ TO THE CAM-CLAY MODEL

In this section, the proposed mechanical quantity $t_{ij}$ will be adapted to the Cam-clay model as an example of its application to the elastoplastic theories of soils. First of all, we assume that the critical state condition in three-dimensional stresses is determined by the following failure criterion based on the SMP (Matsuoka and Nakai, 1974).

$$X_f \equiv (\tau_{\mathrm{SMP}}/\sigma_{\mathrm{SMP}})_f = \mathrm{const.} \qquad (13)$$

Here subscript $f$ denotes the failure condition. Then, if it is assumed that at any critical state condition under a triaxial compression a soil element undergoing shear distortion deforms without further change in plastic volumetric strain as mentioned in the Cam-clay model, the stress ratio $X_f \equiv (\tau_{\mathrm{SMP}}/\sigma_{\mathrm{SMP}})_f$ and the plastic strain increment ratio $Y_f \equiv (d\varepsilon_{\mathrm{SMP}}^*/d\gamma_{\mathrm{SMP}}^*)_f$ at the critical state are expressed as follows by the major-minor principal stress ratio at failure under triaxial compression, $R_f \equiv (\sigma_1/\sigma_3)_{f\ (\mathrm{comp.})}$,

$$X_f = (\sqrt{2}/3)\cdot(\sqrt{R_f} - \sqrt{1/R_f}) \qquad (14)$$

$$Y_f = (1-\sqrt{R_f})/\{\sqrt{2}(\sqrt{R_f}+0.5)\} \qquad (15)$$

The above equations are obtained from Eqs. (3) to (6) under the condition that $\sigma_2 = \sigma_3$, $d\varepsilon_2^p = d\varepsilon_3^p$ and $d\varepsilon_v^p = d\varepsilon_1^p + d\varepsilon_2^p + d\varepsilon_3^p = 0$ at $\sigma_1/\sigma_3 = R_f$. In this paper superscripts $p$ and $e$ denote the plastic and elastic components, respectively.

The equation of energy dissipation in the original Cam-clay model was expressed as follows (Roscoe et al., 1963; Schofield and Wroth, 1968),

$$\begin{aligned} dW_{ex} &\equiv \sigma_1\cdot d\varepsilon_1^p + \sigma_2\cdot d\varepsilon_2^p + \sigma_3\cdot d\varepsilon_3^p \\ &= p\cdot d\varepsilon_v^p + q\cdot d\varepsilon_d^p \\ &= dW_{in} \equiv M\cdot p\cdot d\varepsilon_d^p \end{aligned} \qquad (16)$$

Here $p = (1/3)\cdot(\sigma_1+\sigma_2+\sigma_3)$, $q = (1/\sqrt{2})\cdot\{(\sigma_1-\sigma_2)^2 + (\sigma_2-\sigma_3)^2 + (\sigma_3-\sigma_1)^2\}^{1/2}$, $d\varepsilon_v^p = d\varepsilon_1^p + d\varepsilon_2^p + d\varepsilon_3^p$, $d\varepsilon_d^p = (\sqrt{2}/3)\cdot\{(d\varepsilon_1^p - d\varepsilon_2^p)^2 + (d\varepsilon_2^p - d\varepsilon_3^p)^2 + (d\varepsilon_3^p - d\varepsilon_1^p)^2\}^{1/2}$, $M$ is a soil parameter, $dW_{ex}$ is the irrecoverable energy per unit volume done by the external forces and $dW_{in}$ is the energy per unit volume dissipated in the soil skeleton. Now, if it is assumed that the behavior of soil is fundamentally controlled not by the stress $\sigma_{ij}$ but by the proposed mechanical quantity $t_{ij}$, the relation corresponding to Eq. (16) is given as follows by use of the principal values of $t_{ij}$;

$$\begin{aligned} dW_{ex}^* &\equiv t_1\cdot d\varepsilon_1^p + t_2\cdot d\varepsilon_2^p + t_3\cdot d\varepsilon_3^p \\ &= t_N\cdot d\varepsilon_{\mathrm{SMP}}^{*p} + t_S\cdot d\gamma_{\mathrm{SMP}}^{*p} \\ &= dW_{in}^* \equiv t_N\cdot(Y_f\cdot d\gamma_{\mathrm{SMP}}^{*p}) + X_f\cdot t_N\cdot d\gamma_{\mathrm{SMP}}^{*p} \\ &= M^*\cdot t_N\cdot d\gamma_{\mathrm{SMP}}^{*p} \quad (M^* = X_f + Y_f) \end{aligned} \qquad (17)$$

From Eq. (17), the following relation between the stress ratio and the plastic strain increment ratio can be obtained.

$$\frac{d\varepsilon_{\mathrm{SMP}}^{*p}}{d\gamma_{\mathrm{SMP}}^{*p}} = M^* - \frac{t_S}{t_N} \qquad (18)$$

On the other hand, if we apply the same idea to the modified Cam-clay model of Roscoe and Burland (1968), we can obtain the following relation between the stress ratio and the plastic strain increment ratio, which corresponds to $d\varepsilon_v^p/d\varepsilon_d^p = \{M^2 - (q/p)^2\}/\{2(q/p)\}$ in the modified Cam-clay model.

$$\frac{d\varepsilon_{\mathrm{SMP}}^{*p}}{d\gamma_{\mathrm{SMP}}^{*p}} = \frac{X_f^2 - (t_S/t_N)^2}{2(t_S/t_N)} + Y_f \qquad (19)$$

The broken line with dots and the solid line in Fig. 3 represent the relations between $X \equiv t_S/t_N$ and $Y \equiv d\varepsilon_{\mathrm{SMP}}^{*p}/d\gamma_{\mathrm{SMP}}^{*p}$ of Eqs. (18) and (19), respectively, where $X_f = 0.63$ and $Y_f = -0.26$ are the values determined for the Fujinomori clay which will be described in the next section.

Next, since the void ratio $e$ of a normally consolidated clay is determined only by the current stress condition and is not affected by the past stress history (Henkel, 1960), we regard the plastic volumetric strain $\varepsilon_v^p$ as the strain hardening parameter. Then $\varepsilon_v^p$ can be given by the following equation

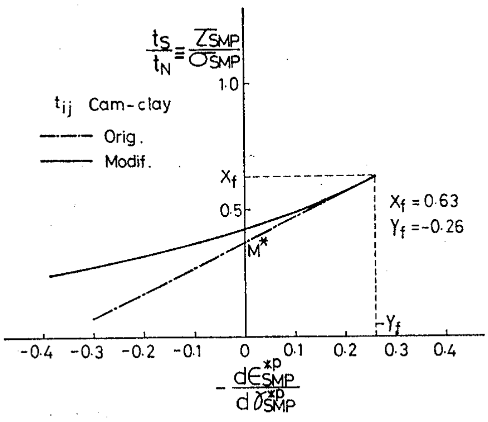


**Fig. 3. Proposed relation between the stress ratio ($t_S/t_N$) and the plastic strain increment ratio ($d\varepsilon_{SMP}{}^{*p}/d\gamma_{SMP}{}^{*p}$)**

under a constant stress ratio condition (e. g., isotropic consolidation and $K_0$-consolidation), in the same manner as in the Cam-clay model.

$$\varepsilon_v{}^p=\frac{\lambda-\kappa}{1+e_0}\ln\frac{t_N}{t_{N0}}\left(=\frac{\lambda-\kappa}{1+e_0}\ln\frac{p}{p_0}\right) \quad (20)$$

Here $p$ is the effective mean principal stress, $e_0$ is the initial void ratio at $t_S=0$ and $t_N=t_{N0}(=p_0)$, $\lambda$ is the compression index $(=0.434\,C_c)$ and $\kappa$ is the swelling index $(=0.434\,C_s)$.

If it is assumed that the directions of the principal axes of $t_{ij}$ coincide with those of the plastic principal strain increments and that the associated flow rule holds in the space of $t_{ij}$ as shown in Fig. 4, the following normality condition is obtained.

$$dt_1\cdot d\varepsilon_1{}^p+dt_2\cdot d\varepsilon_2{}^p+dt_3\cdot d\varepsilon_3{}^p$$
$$=dt_N\cdot d\varepsilon_{SMP}{}^{*p}+dt_S\cdot d\gamma_{SMP}{}^{*s}$$

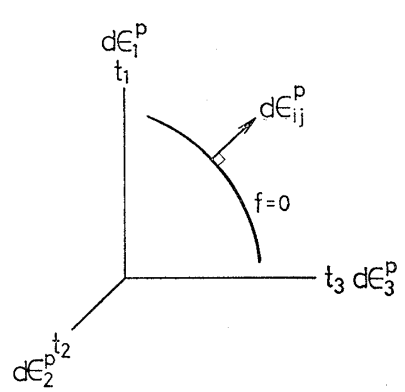


**Fig. 4. Associated flow rule in the $t_{ij}$ space**

$$=0 \quad (21)$$

Solving the differential equation which is derived by combining Eq. (18) or (19) with Eq. (21), and then considering Eq. (20) to eliminate the integral constant, we can eventually obtain the following yield functions in terms of $t_{ij}$.

In the case of the original model:

$$f=\frac{\lambda-\kappa}{1+e_0}\left[\ln\frac{t_N}{t_{N0}}+\frac{X}{M^*}\right]-\varepsilon_v{}^p=0 \quad (22)$$

In the case of the modified model:

$$f=\frac{\lambda-\kappa}{1+e_0}\left[\ln\frac{t_N}{t_{N0}}+\int_0^X\frac{2X\cdot dX}{X^2+2Y_f\cdot X+X_f{}^2}\right]$$
$$-\varepsilon_v{}^p=0 \quad (X\equiv t_S/t_N) \quad (23)$$

From Eq. (22) or (23), the plastic strain increment tensor $d\varepsilon_{ij}{}^p$ is given as follows, since the direction of plastic strain increment is normal to the yield surface in the space of $t_{ij}$:

$$d\varepsilon_{ij}{}^p=\Lambda\frac{\partial f}{\partial t_{ij}} \quad (24)$$

A way to calculate $\partial f/\partial t_{ij}$ in terms of $\sigma_{ij}$ is shown in Appendix 1. Here, since the yield function is given in the form of $f(t_{ij},\ a_i,\ \varepsilon_v{}^p)=f(\sigma_{ij},\ \varepsilon_v{}^p)=0$, the total differential form of the yield function is expressed as

$$df=\frac{\partial f}{\partial\sigma_{ij}}d\sigma_{ij}+\frac{\partial f}{\partial\varepsilon_v{}^p}\cdot\frac{\partial\varepsilon_v{}^p}{\partial\varepsilon_{ij}{}^p}d\varepsilon_{ij}{}^p=0 \quad (25)$$

By combining Eqs. (24) and (25), the proportionality constant $\Lambda$ is expressed as

$$\Lambda=\frac{-\dfrac{\partial f}{\partial\sigma_{ij}}\cdot d\sigma_{ij}}{\dfrac{\partial f}{\partial\varepsilon_v{}^p}\cdot\dfrac{\partial\varepsilon_v{}^p}{\partial\varepsilon_{kl}{}^p}\cdot\dfrac{\partial f}{\partial t_{kl}}} \quad (26)$$

The elastic strain increment tensor $d\varepsilon_{ij}{}^e$ is given by use of generalized Hooke's law

$$d\varepsilon_{ij}{}^e=\frac{1+\nu_e}{E_e}d\sigma_{ij}-\frac{\nu_e}{E_e}d\sigma_{kk}\cdot\delta_{ij} \quad (27)$$

where $\delta_{ij}$ is the Kronecker delta and $E_e$ is expressed in terms of the swelling index $\kappa$ and the Poisson's ratio $\nu_e$ as

$$E_e=\frac{3(1-2\nu_e)(1+e_0)p}{\kappa} \quad (28)$$

Therefore, the total strain increment tensor $d\varepsilon_{ij}$ is given by

$$d\varepsilon_{ij}=d\varepsilon_{ij}^{p}+d\varepsilon_{ij}^{e} \qquad (29)$$

## COMPARISON OF ANALYTICAL RESULTS WITH EXPERIMENTAL RESULTS

Saturated remoulded normally consolidated Fujinomori clay was used in the experiment. Physical properties of the clay are as follows: the liquid limit $w_L=44.7\%$, the plastic limit $w_P=24.7\%$ and the specific gravity $G_s=2.65$. The specimens were prepared by one-dimensionally consolidating the clay mixed with deaired water under a pressure of 49 kN/m$^2$ and forming this consolidated clay in the shape of cylinders of 3.5 cm in diameter and 8 cm in height. The initial water content of the specimens was approximately 40%. Six types of shear tests were performed; constant mean principal stress tests ($\sigma_m=196$ kN/m$^2$), constant minor principal stress tests ($\sigma_3=196$ kN/m$^2$) and undrained tests (initial effective confining pressure $p_0=196$ kN/m$^2$) under triaxial compression and extension conditions. A back pressure of 98 kN/m$^2$ was applied to the specimens in the undrained shear tests.

All the soil parameters of the Fujinomori clay are listed in Table 1. Here, $\lambda/(1+e_0)$ and $\kappa/(1+e_0)$ are determined from an isotropic consolidation test and $R_f\equiv(\sigma_1/\sigma_3)_{f(\mathrm{comp.})}$ is determined from a conventional triaxial compression test in the same manner as in the Cam-clay model. Then, $X_f$ and $Y_f$ are estimated from Eqs. (14) and (15), and we obtained $X_f=0.62$ and $Y_f=-0.26$. The Poisson's ratio $\nu_e$ is assumed to be 0.3. On the other hand, since the original model of Eq. (22) overpredicted the strain increments for changes in stress ratio at a low stress ratio in the same way as the original Cam-clay model, comparisons are shown here

**Table 1. Soil parameters for Fujinomori clay used in analysis**

| | |
|---|---|
| $\lambda/(1+e_0)$ | $5.078\times10^{-2}$ |
| $\kappa/(1+e_0)$ | $0.694\times10^{-2}$ |
| $R_f$ | 3.5 |
| $\nu_e$ | 0.3 |

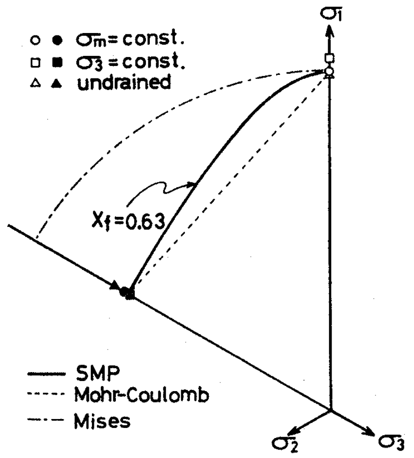


**Fig. 5. Critical state condition based on the SMP on the octahedral plane**

between the observed values and the values predicted by the modified model of Eq. (23). The model in which $t_{ij}$ is applied to the Cam-clay model is named "$t_{ij}$ Cam-clay model" in this paper. The summaries of the "Cam-clay model (modif.)" and the "$t_{ij}$ Cam-clay model (modif.)" are tabulated in Appendix 2.

Fig. 5 shows the critical state condition based on the SMP ($X_f=0.63$) and the stress conditions at failure obtained by the six shear tests on the octahedral plane. The open and solid dots denote experimental results under triaxial compression and extension conditions respectively. In this figure, Mohr-Coulomb's criterion and extended Mises's criterion employed in the Cam-clay model are also described. Although shear tests under three different principal stresses are not performed, the criterion based on the SMP has a good correspondence to the experimental results on clay by Shibata and Karube (1965).

Fig. 6 shows results of the constant mean principal stress tests under triaxial compression and extension conditions with respect to the relation between $t_S/t_N\equiv\tau_{SMP}/\sigma_{SMP}$ and $d\varepsilon_{SMP}^*/d\gamma_{SMP}^*$, together with the theoretical line of Eq. (19). It is seen from this figure that the both test results are uniquely arranged in this relation and that Eq. (19) is appropriate. In Fig. 7, these experimental results and theoretical values are rearranged with respect to the relation between $q/p$

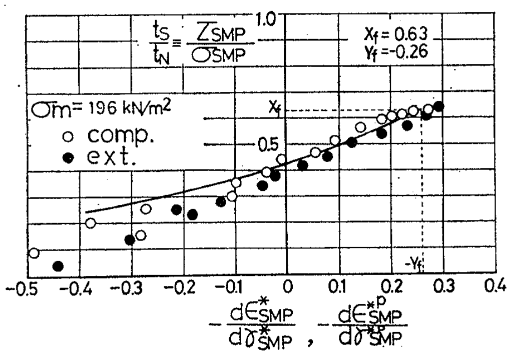


**Fig. 6. Relation between $t_S/t_N$ and $d\varepsilon_{SMP}^*/d\gamma_{SMP}^*$ in constant mean principal stress tests**

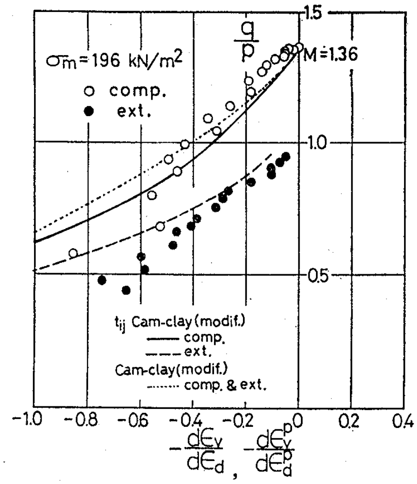


**Fig. 7. Relation between $q/p$, and $d\varepsilon_v/d\varepsilon_d$ in the same tests as Fig. 6**

and $d\varepsilon_v/d\varepsilon_d$ ($d\varepsilon_v^p/d\varepsilon_d^p$ in the case of theoretical values), according to the Cam-clay model. The dotted line, which represent the relation in the modified Cam-clay model, cannot explain such a difference between triaxial compression and extension conditions as is seen in the experimental results and the theoretical values of Eq. (19).

Fig. 8 compares the observed values (dots) of the triaxial compression and extension tests ($\sigma_m=196\,\mathrm{kN/m^2}$) with the results calculated by the $t_{ij}$ Cam-clay model and the Cam-clay model in terms of the relation among $q/p$, $\varepsilon_d$ and $\varepsilon_v$. Though the analytical curve by the Cam-clay model (dotted lines) has a good estimate under triaxial compression conditions, it does not describe the behavior of clay under triaxial extension condition well.

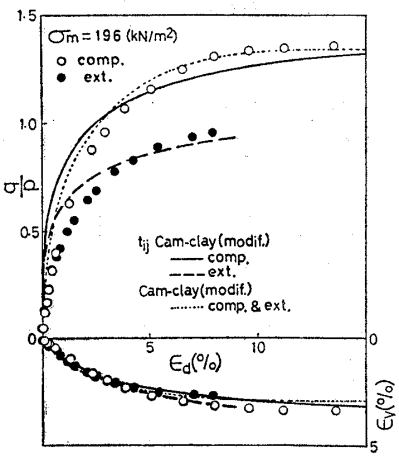


**Fig. 8. Relation among $q/p$, $\varepsilon_d$ and $\varepsilon_v$ in constant mean principal tests**

Figs. 9(a)-(e) show analytical results of true triaxial tests ($\theta=0°$, 15°, 30°, 45° and 60°) by the proposed model with respect to the relation between the principal stress ratio $\sigma_1/\sigma_3$ and the principal strains ($\varepsilon_1$, $\varepsilon_2$ and $\varepsilon_3$). Here, $\theta$ represents the angle of radial stress path from $\sigma_1$ direction on the octahedral plane ($\theta=0°$ and 60° correspond to the triaxial compression and triaxial extension conditions respectively). It is apparent from Figs. 9(a)-(e) that the stress condition at failure in plane strain tests exists between $\theta=15°$ and $\theta=30°$, because the intermediate principal strain $\varepsilon_2$ is expansive at $\theta=15°$ and is compressive at $\theta=30°$. Fig. 10 shows the direction of the plastic strain increment predicted by the proposed model as vectors on the octahedral plane. The directions of the calculated strain increment vectors on the octahedral plane deviate from those of the corresponding deviatoric stress vectors with a definite trend as the stress ratio increases under the three different principal stresses ($\theta=15°$, 30° and 45°). This tendency of the analytical results corresponds to that of the test results on clay by Yong and Mckeys (1971). The Cam-clay model, however, cannot explain such a deviation between the strain increment and the stress in direction.

Figs. 11 and 12 show analytical results by the proposed model (solid and broken lines) and the observed values (plots) of triaxial

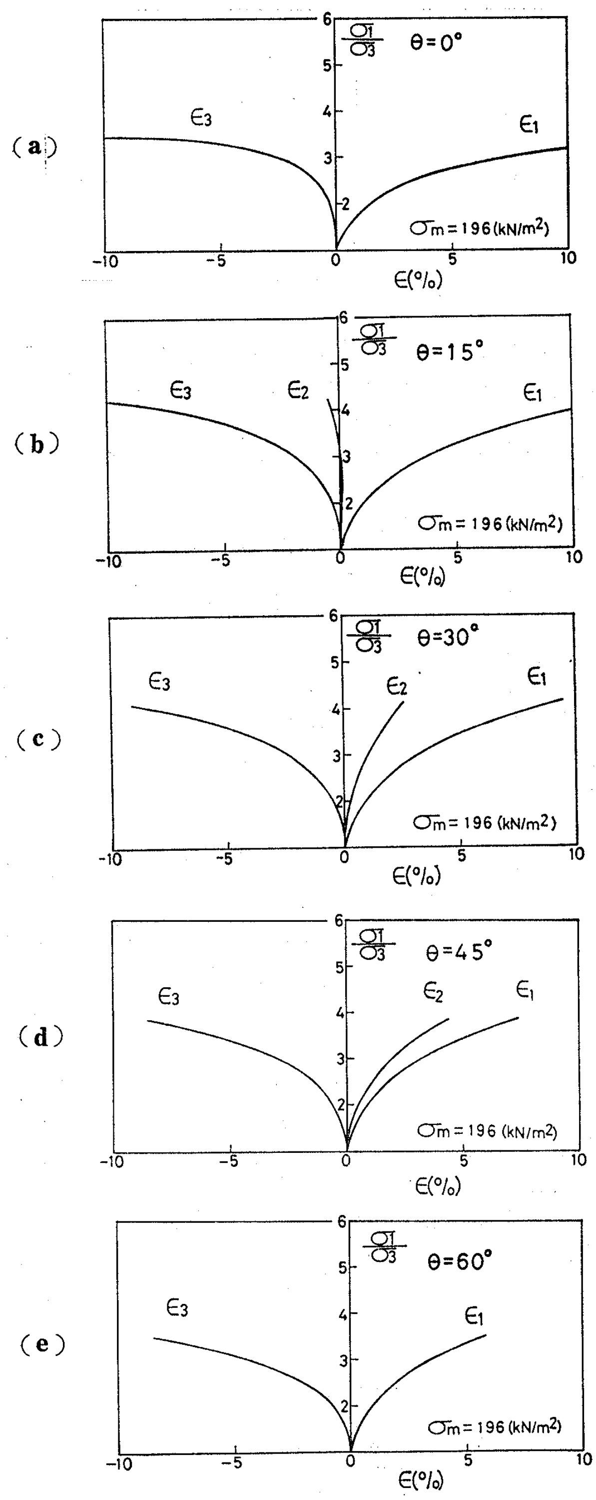


**Fig. 9. Calculated principal stress ratio vs. principal strains in true triaxial tests ($\theta=0°$, 15°, 30°, 45° and 60°)**

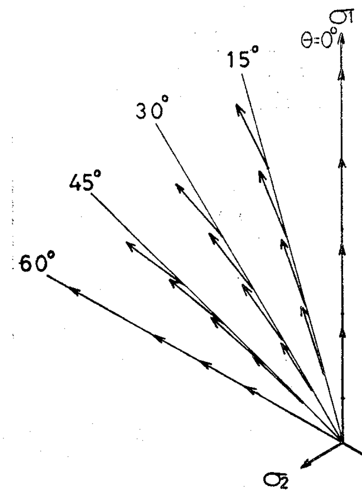


**Fig. 10. Directions of calculated strain increments on the octahedral plane in true triaxial tests**

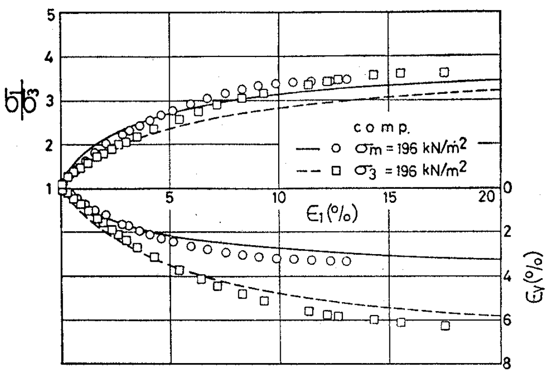


**Fig. 11. Major principal strain vs. principal stress ratio and volumetric strain in triaxial compression tests**

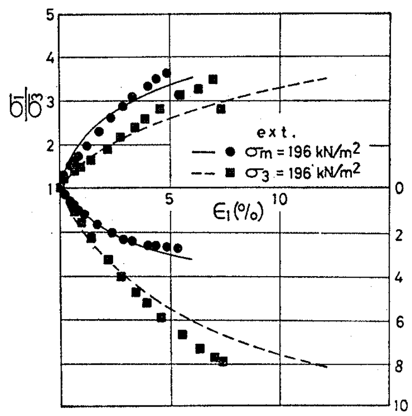


**Fig. 12. Major principal strain vs. principal stress ratio and volumetric strain in triaxial extension tests**

compression and extension tests, respectively, in terms of the relation among $\sigma_1/\sigma_3$, $\varepsilon_1$ and $\varepsilon_v$. The solid curves and circular dots represent the results of the constant mean principal stress tests, and the broken curves and quadrilateral marks represent the results of the constant minor principal stress

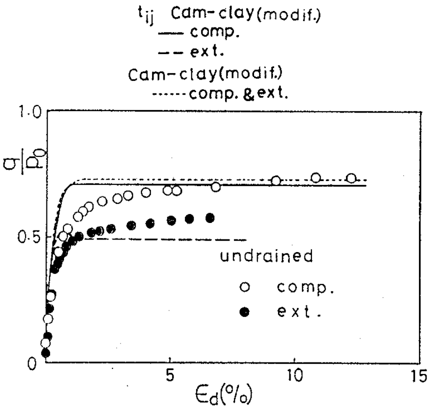


**Fig. 13. Stress-strain relationship in undrained triaxial compression and extension tests**

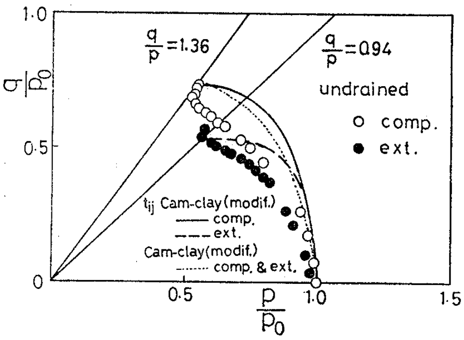


**Fig. 14. Effective stress paths in undrained triaxial compression and extension tests**

tests. It is obvious that the proposed model well describes the shear behavior of clay under the stress path with increase in mean principal stress as well as under the constant mean principal stress.

Figs. 13 and 14 show the stress-strain relationship and the effective stress paths of the undrained shear tests respectively. In these figures, $p_0$ denotes the confining pressure before shear. Analytical results (solid and broken lines) by the proposed model account for the observed differences between triaxial compression and triaxial extension tests, though the dotted lines by the Cam-clay model do not.

Fig. 15 shows analytical results of triaxial compression, triaxial extension and plane strain tests under constant minor principal stress ($\sigma_3=196\,\mathrm{kN/m^2}$) in terms of the relation between $\sigma_1/\sigma_3$ and ($\varepsilon_1$ and $\varepsilon_3$). In this figure each end of the calculated curves

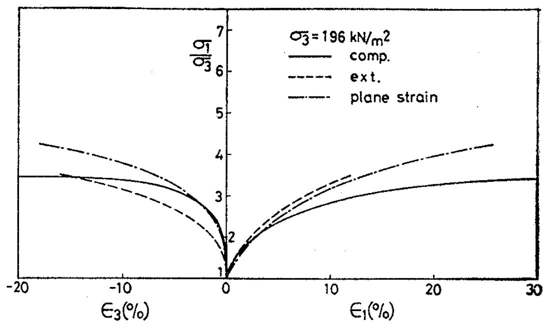


**Fig. 15 Calculated stress-strain curves in triaxial compression, triaxial extension and plane strain tests under a constant minor principal stress**

represents the stress condition at failure which is determined by the criterion based on the SMP in Fig. 5. It is seen from Fig. 15 that while the stress ratio at failure ($(\sigma_1/\sigma_3)_f$) under both triaxial compression and extension conditions is 3.5, the ratio $(\sigma_1/\sigma_3)_f$ under the plane strain condition is 4.24 and is greater than that under triaxial conditions.

Finally, let us analyze pure shear tests in order to check the validity of the proposed model when the principal stress axes rotate. As shown in Fig. 16, a state of pure shear is produced by applying a shear stress increment $\Delta\tau_{xy}$ to an element gradually under the condition that normal stresses $\sigma_x$, $\sigma_y$ and $\sigma_z$ are kept constant.

Analytical results are shown in Fig. 17 with respect to the relation among $\tau_{xy}/\sigma_{m0}$, $\gamma_{xy}$ and $\varepsilon_v$, where $\sigma_{m0}$ denotes the mean principal stress before and during shear. In this figure, the solid lines represent the results on the clay after $K_0$-consolidation ($K_0$ value is assumed to be 0.5) and the

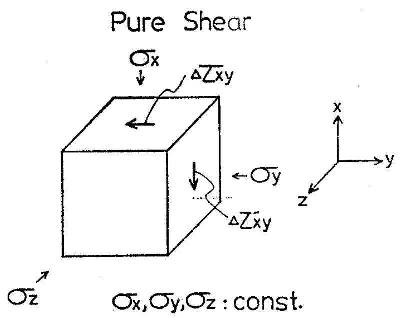


**Fig. 16. Diagram for explanation of pure shear condition**

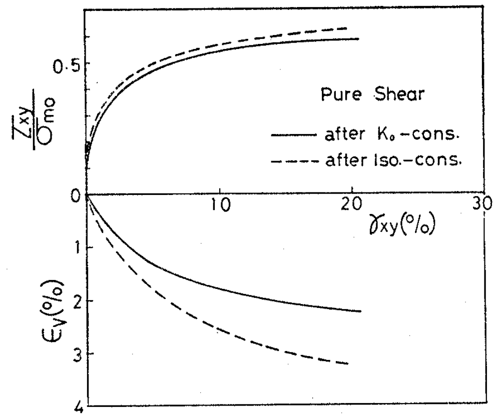


**Fig. 17. Calculated stress-strain curve in pure shear tests on samples after $K_0$-consolidation and isotropic consolidation**

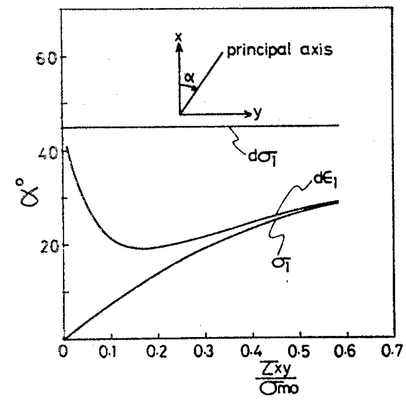


**Fig. 18. Calculated directions of the major principal axes of the strain increment, the stress and the stress increment in pure shear test on sample after $K_0$-consolidation**

broken lines the results after isotropic consolidation. Fig. 18 shows the analytical directions of axes of the major principal strain increment ($d\varepsilon_1$), the major principal stress ($\sigma_1$) and the major principal stress increment ($d\sigma_1$) in the pure shear test on the sample after $K_0$-consolidation. It appears that the direction of $d\varepsilon_1$ is between the direction of $\sigma_1$ and the direction of $d\sigma_1$ at a low stress level but converges to the direction of $\sigma_1$ as the stress level increases. This tendency is due to the fact that as the shear stress $\tau_{xy}$ increases, the plastic strain becomes large in comparison with the elastic strain. This is because it is assumed in analysis that the direction of the principal axes of the plastic strain increment, the principal stress and $t_{ij}$ coincide, and the elastic strain increment and the stress increment have the same principal axes. It is obvious from this figure that the analysis here holds even when the principal stress axes rotate.

## CONCLUSIONS

The main results of this paper are summerized as follows:

(1) A new mechanical quantity $t_{ij}$ is proposed by reconsidering the concept of the extended "Spatial Mobilized Plane" (briefly SMP*) which has been introduced in order to analyze the mechanical behavior of soils in three-dimensional stresses. Here, the mechanical quantity is a symmetrical tensor whose principal values are $t_i=\sigma_i \cdot a_i (i=1, 2, 3)$, where $\sigma_i$ is the principal stresses and $a_i$ the direction cosines of the SMP, and the principal axes of $t_{ij}$ and the stress tensor coincide.

(2) The mechanical quantity $t_{ij}$ is applied to the Cam-clay model which is one of the simplest elastoplastic constitutive models for soils. According to the Cam-clay model, the behavior of soils in triaxial extension conditions and/or three different principal stress conditions cannot be analyzed on the basis of the values of soil parameters obtained from tests in triaxial compression conditions. However, the $t_{ij}$ Cam-clay model proposed here can appropriately describe the soil behaviors in general stress conditions involving the unified soil parameters. The soil parameters in the proposed model are the same as those in the primary model. The validity of the proposed model is confirmed by the results of drained and undrained shear tests on normally consolidated clay under triaxial compression and triaxial extension conditions and comparison with the true triaxial tests reported before.

Although in the present paper the mechanical quantity $t_{ij}$ is adapted to the Cam-clay model alone as an example, this $t_{ij}$ is applicable to any other elastoplastic constitutive model whose validity has been checked only in triaxial compression conditions, extending it to the model which is valid in three-dimensional stresses.

## ACKNOWLEDGEMENTS

The authors wish to thank Prof. T. Yamauchi and Prof. H. Matsuoka at Nagoya Institute of Technology for their helpful support and discussions. They are also indebted to Mr. Y. Suzuki for his experimental assistance. This study was done by the financial support of Grant-in-Aid for Encouragement of Young Scientists (No. 57750419) from the Ministry of Education, Science and Calture.

## NOTATION

$a_1, a_2, a_3$=direction cosines of the normal of the SMP
$E_e$=tangential Young's modulus in the elastic component
$f$=yield function
$J_1, J_2, J_3$=first, second and third stress invariants
$q=(1/\sqrt{2})\{(\sigma_1-\sigma_2)^2+(\sigma_2-\sigma_3)^2+(\sigma_3-\sigma_1)^2\}^{1/2}$
$R$=major-minor principal stress ratio under triaxial compression condition
$t_1, t_2, t_3$=principal values of the proposed mechanical quantity $(=\sigma_i \cdot a_i \ (i=1,2,3))$
$t_{ij}$=proposed mechanical quantity
$X=\tau_{SMP}/\sigma_{SMP}\equiv t_S/t_N$
$Y=d\varepsilon_{SMP}^*/d\gamma_{SMP}^*$
$d\gamma_{SMP}^*$=parallel component of the principal strain increment vector to the SMP
$d\varepsilon_{ij}$=strain increment tensor
$d\varepsilon_d=(\sqrt{2}/3)\{(d\varepsilon_1-d\varepsilon_2)^2+(d\varepsilon_2-d\varepsilon_3)^2+(d\varepsilon_3-d\varepsilon_1)^2\}^{1/2}$
$d\varepsilon_v$=volumetric strain increment $(=d\varepsilon_1+d\varepsilon_2+d\varepsilon_3)$
$d\varepsilon_{SMP}^*$=normal component of the principal strain increment vector to the SMP
$\theta$=angle of radial stress paths from $\sigma_1$ direction on the octahedral plane
$\kappa$=swelling index $(=0.434\,C_s)$
$\lambda$=compression index $(=0.434\,C_c)$
$M$=soil parameter in the Cam-clay model $(=(q/p)_f$ in normally consolidated clay)
$\nu_e$=Poisson's ratio in the elastic component
$\sigma_{ij}$=stress tensor
$\overset{*}{\sigma}_{ij}$="second stress tensor" difined by Satake (1982)
$\sigma_m\equiv p$=mean principal stress $(=(1/3)(\sigma_1+\sigma_2+\sigma_3))$
$\sigma_{SMP}\equiv t_N$=normal stress on the SMP
$\tau_{SMP}\equiv t_S$=shear stress on the SMP
$\varphi_{ij}$=fabric tensor

subscript
$f$ : at failure condition
0 : at initial condition
(comp.) : under triaxial compression condition

superscript
$e$ : elastic component
$p$ : plastic component

## REFERENCES

1) Henkel, D. J. (1960) : "The relationship between the effective stress and water content in saturated clay," Géotechnique, Vol. 10, pp. 41–54.
2) Matsuoka, H. (1974) : "A microscopic study on shear mechanism of granular materials," Soils and Foundations, Vol. 14, No. 1, pp. 29–43.
3) Matsuoka, H. and Nakai, T. (1974) : "Stress-deformation and strength characteristics of soil under three different principal stresses," Proc., JSCE, No. 232, pp. 59–70.
4) Matsuoka, H. and Nakai, T. (1977) : "Stress-strain relationship of soil based on the SMP," Proc., Specialty Session 9, 9th ICSMFE, pp. 153–162.
5) Nakai, T. (1981) : "Analyses of soil-footing and soil-wall interaction," Proc., 10th ICSMFE, Vol. 2, pp. 205–208.
6) Nakai, T. and Matsuoka, H. (1980) : "A unified law for soil shear behavior under three dimensional stress condition," Proc., JSCE, No. 303, pp. 65–77 (in Japanese).
7) Nakai, T. and Matsuoka, H. (1983 a) : "Shear behaviors of sand and clay under three-dimensional stress condition," Soils and Foundations, Vol. 23, No. 2, pp. 26–42.
8) Nakai, T. and Matsuoka, H. (1983 b) : "Constitutive equation for soils based on the extended concept of "Spatial Mobilized Plane" and its application to finite element analysis," Soils and Foundations, Vol. 23, No. 4, pp. 87–105.
9) Oda, M. (1972) : "The mechanism of fabric changes during compressional deformation of sand," Soils and Foundations, Vol. 12, No. 2, pp. 1–18.
10) Roscoe, K. H. and Burland, J. B. (1968) : "On the generalized stress-strain behaviour of wet clay," Engineering Plasticity, Cambridge Univ. Press, pp. 535–609.

11) Roscoe, K. H., Schofield, A. N. and Thurairajah, A. (1963) : "Yielding of clays in states wetter than critical," Géotechnique, Vol. 13, No. 3, pp. 211-240.
12) Satake, M. (1982) : "Fabric tensor in granular materials," Proc., IUTAM-Conference on Deformation and Failure of Granular Materials, pp. 63-68.
13) Schofield, A. N. and Wroth, C. P. (1968) : Critical State Soil Mechanics, Mcgraw-Hill, London.
14) Shibata, T. and Karube, D. (1965) : "Influence of the variation of the intermediate principal stress on the mechanical properties of normally consolidated clay." Proc., 6th ICSMFE, Vol. 1, pp. 359-363.
15) Yong, R. N. and Mckeys, E. (1971) : "Yield and failure of clay under triaxial stresses," Proc., ASCE, Vol. 97, No. SM 1, pp. 159-176.

## APPENDIX 1

Although the yield function $f$ is given as a function of the principal values of $t_{ij}$ as is seen from Eqs. (8), (9), (22) and (23), the derivative $\partial f/\partial t_{ij}$ can be calculated as follows:

$$\begin{aligned}\frac{\partial f}{\partial t_{ij}}&=\frac{\partial f}{\partial t_k}\cdot\frac{\partial t_k}{\partial t_{ij}}\\&=\left(\frac{\partial f}{\partial t_N}\cdot\frac{\partial t_N}{\partial t_k}+\frac{\partial f}{\partial t_S}\cdot\frac{\partial t_S}{\partial t_k}\right)\cdot\frac{\partial t_k}{\partial t_{ij}}\\&=\left(\frac{\partial f}{\partial t_N}\cdot\frac{\partial t_N}{\partial t_k}+\frac{\partial f}{\partial t_S}\cdot\frac{\partial t_S}{\partial t_k}\right)\cdot\frac{\partial \sigma_k}{\partial \sigma_{ij}}\end{aligned}\qquad \text{(A1)}$$

This is because $t_{ij}$ is a symmetrical tensor written in terms of the stress tensor $\sigma_{ij}$ and the directions of the principal axes of $t_{ij}$ coincide with those of the stress. For example, the derivative $\partial f/\partial t_{ij}$ is calculated as follows under the plane strain condition: In Eq. (A 1), the expressions of $\partial f/\partial t_N$ and $\partial f/\partial t_S$ are obtained from Eq. (22) or (23), and $\partial t_N/\partial t_k$ and $\partial t_S/\partial t_k$ are given on referring to Eqs. (8) and (9) respectively. If we assume that $d\varepsilon_{33}=d\varepsilon_{23}=d\varepsilon_{13}=0$ and $\sigma_{23}=\sigma_{13}=0$, there are following relations between the principal stresses ($\sigma_1$ and $\sigma_2$) and the stresses ($\sigma_{11}$, $\sigma_{22}$, $\sigma_{12}$ and $\sigma_{21}$).

$$\left.\begin{aligned}\sigma_1&=\frac{1}{2}(\sigma_{11}+\sigma_{22})+I^{1/2}\\\sigma_2&=\frac{1}{2}(\sigma_{11}+\sigma_{22})-I^{1/2}\end{aligned}\right\}\qquad \text{(A2)}$$

where

$$I=\left(\frac{\sigma_{11}-\sigma_{22}}{2}\right)^2+\sigma_{12}\sigma_{21}\qquad \text{(A3)}$$

Therefore, the derivative $\partial t_k/\partial t_{ij}=\partial\sigma_k/\partial\sigma_{ij}$ is expressed as,

$$\left.\begin{aligned}&\frac{\partial t_1}{\partial t_{11}}=\frac{\partial t_2}{\partial t_{22}}=\frac{1}{2}+\frac{1}{4}(\sigma_{11}-\sigma_{22})\cdot I^{-1/2}\\&\frac{\partial t_1}{\partial t_{22}}=\frac{\partial t_2}{\partial t_{11}}=\frac{1}{2}-\frac{1}{4}(\sigma_{11}-\sigma_{22})\cdot I^{-1/2}\\&\frac{\partial t_1}{\partial t_{12}}=\frac{1}{2}\sigma_{21}I^{-1/2}\\&\frac{\partial t_2}{\partial t_{12}}=-\frac{1}{2}\sigma_{21}I^{-1/2}\\&\frac{\partial t_3}{\partial t_{33}}=1\end{aligned}\right\}\qquad \text{(A4)}$$

## APPENDIX 2

**Table A1. Comparison between "Cam-clay model (modif.)" and "$t_{ij}$ Cam-clay model (modif.)"**

| constitutive model | Cam-caly (modif.) | $t_{ij}$ Cam-clay (modif.) |
|---|---|---|
| 1. stress parameters and plastic strain increment parameters used in each model | $p=\frac{1}{3}(\sigma_1+\sigma_2+\sigma_3)$<br>$q=\frac{1}{\sqrt{2}}\sqrt{(\sigma_1-\sigma_2)^2+(\sigma_2-\sigma_3)^2+(\sigma_3-\sigma_1)^2}$<br>$d\varepsilon_v{}^p=d\varepsilon_1{}^p+d\varepsilon_2{}^p+d\varepsilon_3{}^p$<br>$d\varepsilon_d{}^p=\frac{\sqrt{2}}{3}\sqrt{(d\varepsilon_1{}^p-d\varepsilon_2{}^p)^2+(d\varepsilon_2{}^p-d\varepsilon_3{}^p)^2+(d\varepsilon_3{}^p-d\varepsilon_1{}^p)^2}$ | $t_N=t_1a_1+t_2a_2+t_3a_3$<br>$t_S=\sqrt{(t_1a_2-t_2a_1)^2+(t_2a_3-t_3a_2)^2+(t_3a_1-t_1a_3)^2}$<br>$d\varepsilon_{SMP}{}^{*p}=d\varepsilon_1{}^p a_1+d\varepsilon_2{}^p a_2+d\varepsilon_3{}^p a_3$<br>$d\gamma_{SMP}{}^{*p}=\sqrt{(d\varepsilon_1{}^p a_2-d\varepsilon_2{}^p a_1)^2+(d\varepsilon_2{}^p a_3-d\varepsilon_3{}^p a_2)^2+(d\varepsilon_3{}^p a_1-d\varepsilon_1{}^p a_3)^2}$ |
| 2. stress ratio-plastic strain increment ratio relation | $d\varepsilon_v{}^p/d\varepsilon_d{}^p=(M^2-\eta^2)/(2\eta),\ \eta\equiv q/p$<br>where, $M\equiv(q/p)_f=3(R_f-1)/(R_f+2)$ | $d\varepsilon_{SMP}{}^{*p}/d\gamma_{SMP}{}^{*p}=(X_f{}^2-X^2)/(2X)+Y_f,$<br>$X\equiv t_S/t_N$<br>where, $X_f=(\sqrt{2}/3)\cdot(\sqrt{R_f}-\sqrt{1/R_f})$<br>$Y_f=(1-\sqrt{R_f})/\{\sqrt{2}(\sqrt{R_f}+0.5)\}$ |
| 3. strain hardening parameter | $\varepsilon_v{}^p$<br>$\left(\begin{array}{l}\varepsilon_v{}^p=\{(\lambda-\kappa)/(1+e_0)\}\ln(p/p_0)\\ \text{under constant stress ratio}\end{array}\right)$ | same as the left |
| 4. yield function | $f=\frac{\lambda-\kappa}{1+e_0}\left[\ln\frac{p}{p_0}+\int_0^{\eta}\frac{2\eta\cdot d\eta}{\eta^2+M^2}\right]-\varepsilon_v{}^p=0$ | $f=\frac{\lambda-\kappa}{1+e_0}\left[\ln\frac{t_N}{t_{N0}}+\int_0^{X}\frac{2X\cdot dX}{X^2+2Y_f\cdot X+X_f{}^2}\right]-\varepsilon_v{}^p=0$ |
| 5. associated flow rule | $d\varepsilon_{ij}{}^p=\Lambda\cdot\frac{\partial f}{\partial\sigma_{ij}}$<br>where, $\Lambda=-\frac{\partial f}{\partial\sigma_{ij}}\cdot d\sigma_{ij}\Big/\left(\frac{\partial f}{\partial\varepsilon_v{}^p}\cdot\frac{\partial\varepsilon_v{}^p}{\partial\varepsilon_{kl}{}^p}\cdot\frac{\partial f}{\partial\sigma_{kl}}\right)$ | $d\varepsilon_{ij}{}^p=\Lambda\cdot\frac{\partial f}{\partial t_{ij}}$<br>whera, $\Lambda=-\frac{\partial f}{\partial\sigma_{ij}}\cdot d\sigma_{ij}\Big/\left(\frac{\partial f}{\partial\varepsilon_v{}^p}\cdot\frac{\partial\varepsilon_v{}^p}{\partial\varepsilon_{kl}{}^p}\cdot\frac{\partial f}{\partial t_{kl}}\right)$ |